

Coplanar Three-Beam X-ray Diffraction Study in TeO₂ Single Crystal Using Synchrotron Radiation

A. E. Blagov^a, M. V. Koval'chuk^{a, b}, V. G. Kohn^{a, b}, E. Kh. Mukhamedzhanov^b,
Yu. V. Pisarevsky^a, and P. A. Prosekov^a

^aShubnikov Institute of Crystallography, Russian Academy of Sciences, Moscow, Russia

^bNational Research Centre "Kurchatov Institute", Moscow, Russia

Received March 10, 2011

Abstract—The results of the first experimental study of coplanar three-beam X-ray diffraction in a paratellurite (TeO₂) single crystal using synchrotron radiation on a Kurchatov synchrotron radiation source are presented. Four cases with (220, 371), (220, 464), (220, 370), and (110, 557) indices have been investigated. In all cases the change of the rocking curve shape of the weak reflection has been observed due to the multibeam interaction resulting in the appearance of two peaks in the reflection curve corresponding to two scattering mechanisms: amplitude and resonance. The origin of the insufficient resolution in the experiments has been considered. It has been shown that the obtained data correspond to the results of the computer simulation.

DOI: 10.1134/S1027451011090059

INTRODUCTION

Multibeam diffraction of the X-ray beams in single crystals is of interest from both the fundamental point of view and in connection with the development and improvement of methods of characterization of the structure of the crystal solid state. Recently in this field a transition has been observed from studies devoted to the observation of the features' multibeam diffraction to the development of multibeam diffraction schemes directed to the study of the structure of ideal and distorted crystals and elaboration of methods of determination of the phases of the structural amplitudes, specification of the interplane distances, and the value of deformations of the crystal lattice.

Multibeam dynamic diffraction of X-ray beams, as a rule, is studied in crystals with a high degree of the perfection of the crystal lattice [1, 2]. Here silicon crystals are the undoubted leader [3]. It was shown in [4] that a paratellurite TeO₂ single crystal (space group $P4_32_12$, $a = 4.810$, $c = 7.613$ Å) is also suitable for the observation of all features of multibeam diffraction described by the theory for perfect crystals. Of particular interest is the case of coplanar diffraction, in which two diffracted beams are observed in the same planes, i.e., there are two (or more) nodes of the inverse lattice on the Ewald sphere [2]. Such diffraction is weakly sensitive to the angular divergence of the incident beam in the plane perpendicular to the scattering plane that simplifies the requirements to the experimental scheme. On the other hand, it is implemented only in the case of a monochromatic beam, i.e., in the case of a definite wavelength of the X-ray radiation. In particular, under conditions close to coplanar diffraction [4], there was a weak difference

between the MoK_{α1} line from the precise value corresponding to coplanar diffraction for the considered reflections.

When a laboratory X-ray tube is used as a radiator, it is difficult to meet the latter condition, since in this case the quasi-monochromatic radiation gives rise to a given wavelength and bremsstrahlung (quasi-continuous spectrum) is of weak intensity. The problem is easily solved when using a source of synchrotron radiation (SR), since all wavelengths are in its spectrum and a monochromator can be easily tuned to any wavelength.

Thus, the experimental implementation of the simulation results for the cases of multibeam coplanar diffraction in a paratellurite single crystal with different degrees of the contribution to scattering determined by the ratio between the intensities of selected reflections under the conditions of the SR station the scheme of which most adequately corresponds to the performed simulation is of particular interest.

EXPERIMENTAL

Experiments were performed on a Precision X-ray Optics (PXO) station [5] located at channel 6.6 of the Kurchatov Synchrotron Radiation Source (KSRS). A schematic of the experiment is shown in Fig. 1. The beam from the rotating magnet of the Sibir'-2 storage ring KSRS passed through a double-crystal monochromator Si(111) without changing its direction. To reduce the angular divergence, the beam was limited by slits with dimensions of 0.1 mm in the vertical (working) direction and 1 mm in the horizontal direction located at a distance of 16 m from the source. The

vertical plane was the plane of coplanar diffraction, since the vertical size of the source is less than the horizontal one.

After the slit, the monochromatized and collimated beam arrived at the studied paratellurite (TeO_2) sample. As a result of the three-beam diffraction, two reflected beams were observed. The TeO_2 crystal was rocking in the scattering plane (the polar angle), and the changing intensity of the diffracted beams was recorded by two detectors. The azimuthal angle of the crystal orientation was also changed jump-like in diffractometry studies with an X-ray tube, and the energy of the incident radiation was usually fixed. However, reflection in the strictly coplanar case does not depend on the azimuthal angle. In an experiment on synchrotron radiation, there is a possibility to tune the monochromator in order to change the energy of the incident beam, as was performed in this experiment.

Four cases of three-beam coplanar diffraction were studied for the calculated pairs of reflections with (220, 371), (220, 464), (220, 370) and (110, 557) indices. It was shown [4] that the second reflection, which is weak, allows one to observe the three-beam interaction at the strong first and coupling reflections (the indices of the latter show the difference between the indices of the second and first reflections [2]). The first strong reflection almost always remains two-beam, and the coupling reflection occurs on the direction of the weak one.

For the first case, coplanar diffraction is implemented at the photon energy $E = 17.461$ keV. The angular dependences of the reflection factor for the weak reflection 371 are shown in Fig. 2a at different values of the energy of the incident photon. The numbers of steps of the energy shift are specified in the figure. The precise value of the step of the energy change is most easily determined not by the rotation angle of the monochromator, but by the shift of the position of the maximum of the curves of the reflection 371. We take the difference between the positions of the maximum between the 15th and 1st curves; divide it by 14, $\tan\theta_B$ (θ_B is the Bragg angle) for the reflection 371; and multiply it by the energy. As a result, we obtain the step on energy $\Delta E = 0.423$ eV ($\Delta\lambda = 0.172 \times 10^{-4}$ Å).

The broadening of the measured experimental curves of the reflection 371 is larger than that of the reflection 220. The curve for the reflection 220 is shown in Fig. 2b: it almost does not change when the energy changes in small limits. As for the curves of the reflection 371 themselves, they also reproduce themselves far away from the three-beam point (the value of the Bragg angle or wavelength of the radiation, at which the conditions of diffraction for the studied pair of the reflections hold simultaneously) on the energy scale, and the change of the energy simply leads to the shift of the maximum of the curve on the angular scale according to the relationship $\Delta\theta = (\Delta E/E)\tan\theta_B$. However, the character of the angular dependence changes noticeably in the three-beam region. The second max-

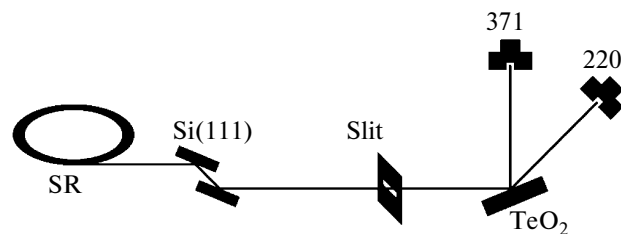


Fig. 1. Experimental schematic: SR is the beam of the synchrotron radiation, Si(111) is a silicon monochromator, and TeO_2 is a sample. Two reflections are recorded by two detectors.

imum arises on the right, while the left-hand maximum decreases. Both maximums are comparable at the definite energy value. Then the right-hand maximum becomes higher and the left-hand one gradually disappears.

Such behavior is related to two mechanisms of reflection at the multibeam diffraction—amplitude and resonance—already described in [4]. These terms were introduced for the first time in [6]. The amplitude mechanism is implemented when the scan angle θ is close to θ_B for a family of planes 220, i.e., the reflection from this family is strong, and there are no conditions for the diffraction of the primary beam for the family of planes {371}. In this case the reflection 220 contributes strongly to the distortion of the form of the curve of the angular dependence of the reflection factor for the reflection 371, since it is determined by the coherent superposition of the incident and the first reflected plane waves. The phase difference between them takes the values from 0 to π at passing the dynamic region of the first reflection. In addition to the amplitude scattering, the effect of the strong reflection on the weak one is also observed outside the three-beam region. This phenomenon is due to virtual or resonance scattering [6]. The effect takes place in a wide angular region as compared with the angular region of the strong reflection and has an asymmetric character. The theory of the resonance scattering is given in [7]. However, in this case, as can be seen in Fig. 2, the resonance mechanism is manifested weakly.

Similar curves are shown in Fig. 3 for the pair of reflections (220, 464). Here coplanar diffraction is implemented almost at the same energy $E = 17.468$ keV, as in the case considered above. Note that when these data are recorded, these data the energy step was $\Delta E = 0.321$ eV ($\Delta\lambda = 0.131 \times 10^{-4}$ Å). It is seen that the strong reflection 220 again remains almost two-beam (shown in Fig. 3b). The curve for this reflection is given in the three-beam region. It almost exactly coincides with the curve for the reflection 371. As to the reflection 464, its angular dependence, when the energy changes, behaves somewhat differently. In this case the resonance scattering turns out to be very strong and it is vividly seen how the height of the two-

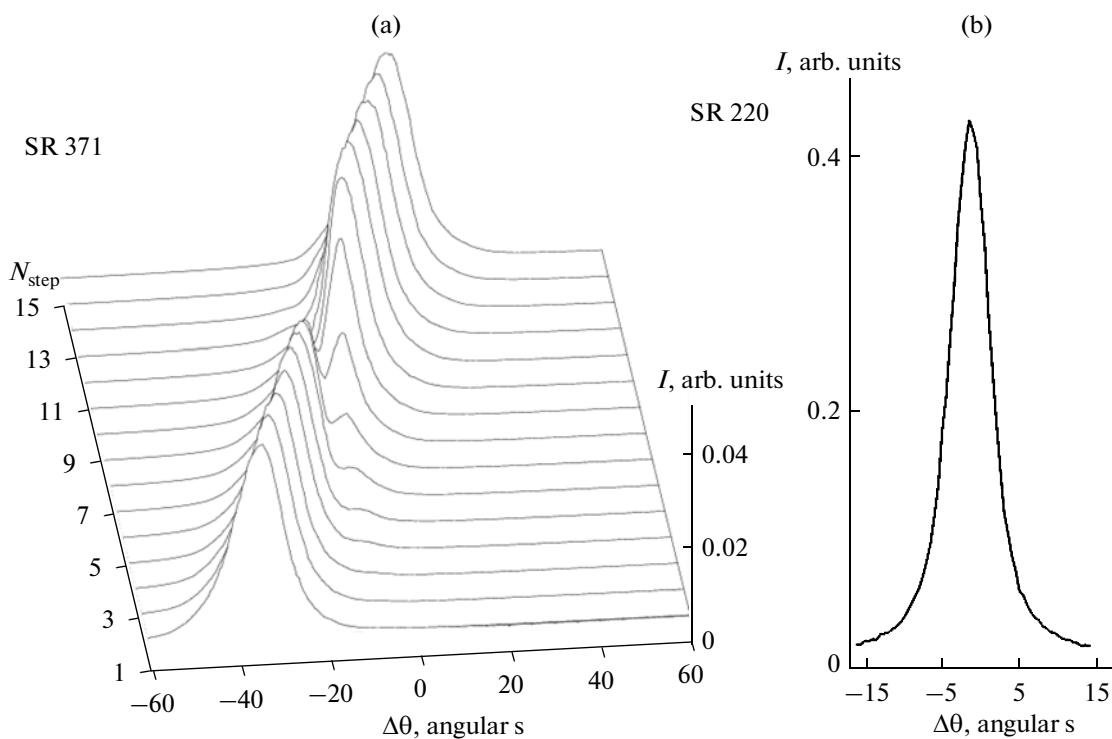


Fig. 2. Experimental curves of the angular dependence of the reflection coefficient of the reflection 371 at different energy values near the three-beam point (a). Numbers on the left-hand axis show the number of steps of the energy photon change. For the strong reflection 220 (b), the curve almost does not depend on the energy change.

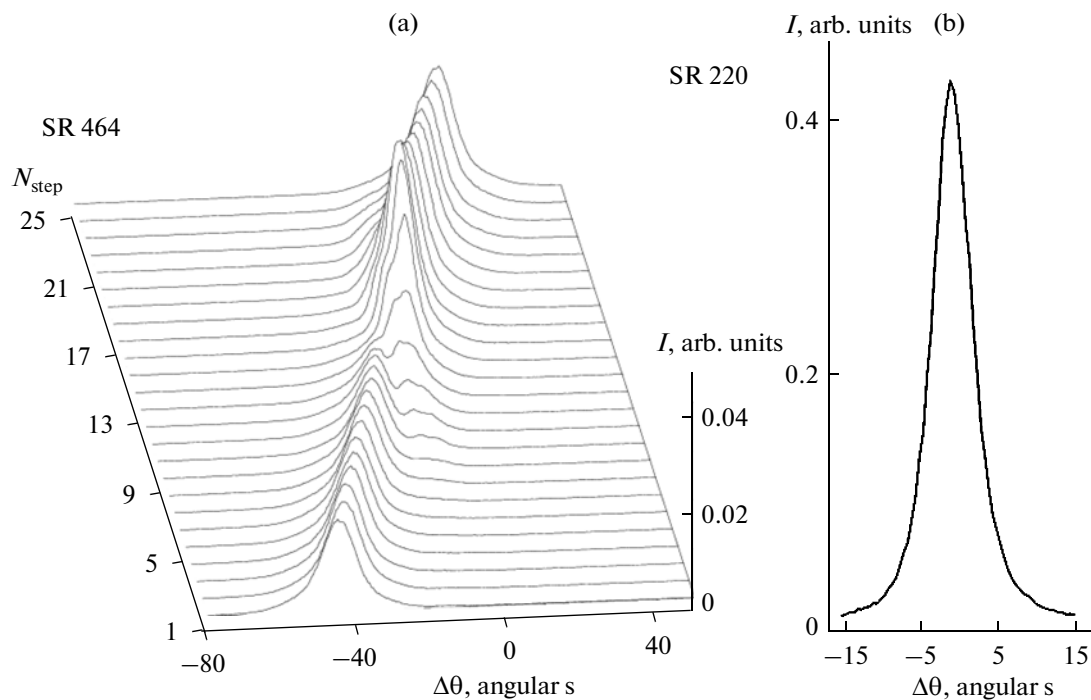


Fig. 3. Experimental curves of the angular dependence of the reflection coefficient of the reflection 371 at the different energy values near the three-beam point (a). Numbers on the left-hand axis show the number of steps of the energy photon change. For the strong reflection 220 (b), the curve almost does not depend the energy change.

beam peak of the reflection decreases in comparison with that of the purely two-beam case at approaching the three-beam point from the left. After passing the three-beam point, the height of the peaks, on the contrary, exceeds the two-beam level. This occurs in the angular region where the intensity of the reflection 220 is small, but its effect is enhanced due to the resonance.

The peak of the amplitude scattering in this case has a feature too. It is split, and it is possible to see a weak minimum in its center. Note that the curves of the reflection 464 are strongly averaged both over the polar angle and the energy and these features only weakly reflect the complex nature of the multibeam interaction.

Coplanar diffraction for reflections (220, 370) is implemented at the close energy $E = 17.695$ keV; however, unlike the reflection 371, here the resonance scattering is also strongly revealed. The obtained experimental curves are similar to those shown in Fig. 3.

Coplanar diffraction for reflections (110, 557) is implemented at the energy $E = 17.452$ keV. The obtained curves closely match the form of the case (220, 371) (Fig. 2), in which the resonance scattering is revealed weakly.

DISCUSSION

The most adequate theoretical approach for the description of the angular and energy dependences obtained in the experiment is the approximation of the plane monochromatic incident wave. In fact, in these experiments, the intensity integral over the detector area is measured, which is equivalent to the integral of the intensity of the reflected beams over the total ensemble of the plane monochromatic waves present in the incident radiation. In other words, integration is performed over the incidence angle and the interval of the photon energy. An ideal variant is such as which the incident radiation is quite strongly collimated and monochromatized.

Thus, to describe the experimental curves, it is necessary to perform integration according to the formula

$$\langle I_{hkl} \rangle(\theta, E) = \int d\theta_1 P(\theta_1) \int dE_1 Q(E_1) I_{hkl}(\theta + \theta_1, E + E_1), \quad (1)$$

where $P(\theta_1)$ and $Q(E_1)$ are the weight functions with the maximum at the zero argument decreasing at infinity and the function $I_{hkl}(\theta, E)$ describes the angular and energy dependence of the intensity of the reflection of the plane incident waves at the angular (θ) and energy (E) deviation from the three-beam point. The reflection occurs from the atomic planes with the Miller indices hkl . The better the weight function is localized, the better results of the experiment are described by the diffraction theory in the approximation of the plane monochromatic wave, and the multibeam interaction is revealed in more details.

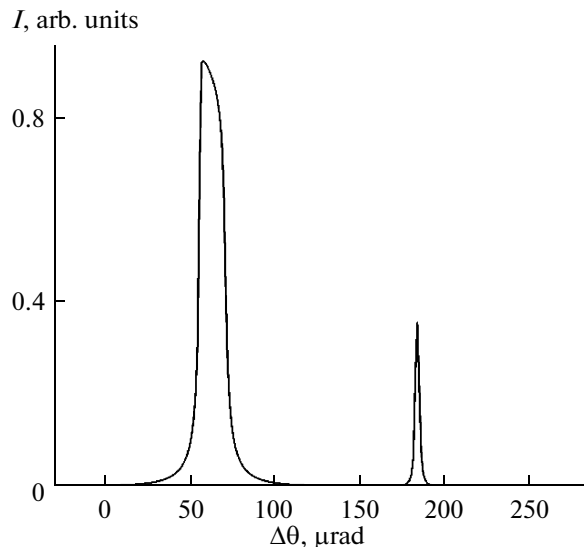


Fig. 4. Theoretical two-beam curves of the reflections 220 and 371 for a plane monochromatic incident wave calculated according to the program of the multibeam calculations far from the region of multibeam diffraction.

Only the polar angle is specified in Eq. (1); i.e., the angle in the scattering plane. The dependence on the azimuthal angle is very weak, and if the incident beam is even slightly collimated on the azimuthal angle, it is possible not to consider it. The weight functions themselves are usually determined from the analysis of the experimental scheme. However, this is always a complicated problem. In most cases collimation and monochromatization of the beam are performed by means of several crystals installed in the scattering scheme [3]. In this case the widths of the weight function are determined from the calculation of the reflection from all crystals of a multicrystal monochromator.

In this experiment the determination of the type and width of the weight function is complicated by the fact that only one crystal-monochromator was used (in fact, two crystals, which in the nonscattering scheme work as one crystal) and a comparatively narrow slit with the size of 100 μm . The theoretical two-beam curves (far from the multibeam point) calculated in the approximation of the plane monochromatic wave for the case (220, 371) are shown in Fig. 4. A standard computer program was used for the multibeam calculations and the method of the calculation is described in [8]. It is seen that the reflection factor for the strong reflection 220 is nearly unity in the region of the total reflection and has a noticeable width. As to the weak reflection 371, it does not completely approach the dynamic mode and its maximum does not reach the value of 0.4. This means that it is semikinematic reflection, in which the extinction length is higher than the absorption length. However, this peak is still very narrow and its width is tenfold lower than the width of the reflection 220.

On the contrary, the width of the weak reflection 371 in the experiment is several times higher than the width of the strong reflection and is $70 \mu\text{rad}$, while its reflection maximum is a tenth as large. This means that in Eq. (1) the weight functions have a definite width and their width for the weak reflection is larger than that for the strong one. It is necessary to understand how these weight functions are formed in this experimental scheme. For a point source and narrow slit, the weight function would have the form of a rectangle. Accordingly, a strongly broadened reflection curve for the weak reflection also would give the form of a rectangle.

However, the Gauss form of the profiles of the experimental peaks in Figs. 2–3 indicates that the main and visible mechanism of the averaging of the experimental curves is the comparatively large size of the source at the KSRS. In fact, the bunch of electrons on the orbit of the storage ring has a density that is distributed according to the Gauss law. This leads to the Gauss distribution of the source brightness, and the halfwidth of this distribution is approximately $160 \mu\text{m}$. Accordingly, the angular size of the Gauss source at the distance of 16 m is about $\Delta\theta_M = 10 \mu\text{rad}$. The obtained angular interval at the reflection from the monochromator leads to the energy scatter of $\Delta E = E\Delta\theta_M \cot\theta_B$, where the Bragg angle corresponds to the reflection 111 in silicon for the given energy. By substituting definite values $E = 17.46 \text{ keV}$, $\theta_B = 6.501^\circ$, we obtain $\Delta E = 1.53 \text{ eV}$.

The energy scatter leads, in turn, to the broadening of the angular dependence of the reflectivity from the sample due to the shift of the reflection maximum according to the formula $\Delta\theta_S = (\Delta E/E)\tan\theta_B$. By substituting the value of the Bragg angle for the reflection 371 in paratellurite, $\theta_B = 34.34^\circ$ and we find $\Delta\theta_S = 60 \mu\text{rad}$. Another $10 \mu\text{rad}$ are added due to the direct angular convergence of the beam, and as a result we obtain the experimental value for the halfwidth of the maximum and the correct form of the reflection profile.

The calculation was performed taking into account the averaging of the theoretical curve with the Gauss weight functions and given halfwidths. The form of the curves of the reflections 220 and 371 obtained as a result of the calculation completely coincides with that of the experimental curves.

In this respect the note that a scheme with one double monochromator on the SR source is not effective enough. The energy and angular resolution of recording can be considerably increased by using two double monochromators located in the scattering scheme. The crystals with the highest possible reflection indices should be used, as it was shown in [3]. Note that it is planned to perform such experiments at the KSRS.

Nevertheless, even under conditions of insufficiently high energy resolution, it was possible to record

experimentally the noticeable difference of the degree of the resonance scattering between the (220, 371) and (220, 464) cases in paratellurite. As it was shown in [4], the renormalization of the parameter of the dynamic two-beam diffraction for the second (371 or 464) reflection due to the resonance scattering is determined by the expression

$$g_{20} = \chi_{20} \left(1 + \frac{C}{\alpha_1} \right), \quad C = \frac{\chi_{21}\chi_{10}}{\chi_{20}}. \quad (2)$$

Here χ_{mm} are the parameters of the two-beam diffraction, the indices 10 correspond to the reflection 220, and the indices 21 correspond to the connecting reflection (151 or 244). The parameter α_1 determines the deviation from the Bragg condition for the first reflection 220. It is expected that it has a sufficiently larger value; i.e., the first reflection in this region has a small intensity.

The direct calculation of the complex factor C gives the following values:

$$C = -(5.01 + 0.74 i) \times 10^{-6} \text{ for the reflection 371;} \\ C = -(10.60 + 1.09 i) \times 10^{-6} \text{ for the reflection 464.}$$

In the second case, the coefficient C is twice as large as that in the first case. This explains the stronger manifestation of the resonance scattering in the case of (220, 464). The paratellurite crystal has a rather complex structure; therefore, the definite value of the Fourier components of the crystal polarizability does not depend so directly on the Miller indices as in the case of silicon crystal.

CONCLUSIONS

Thus, in this work for the first time the three-beam coplanar diffraction in a paratellurite single crystal was studied using the Kurchatov SR source. The obtained data and results of the performed theoretical simulation correspond to each other: the form of the experimental curves coincides completely with the calculated one. The resonance scattering is revealed far away from the region of the three-beam interaction and has an asymmetric character. In all four implemented cases of three-beam interaction, the ratios of the reflection coefficients (strong and weak reflections) were close. However, in the two studied cases, the resonance mechanism was revealed to a greater degree, as confirmed by the theory.

ACKNOWLEDGMENTS

This study was supported by the Ministry of Education and Science of the Russian Federation (GK no. 16.740.11.0095), Russian Foundation for Basic Research (project no. 10-02-00047a), and President of the Russian Federation (grant no. MK-156.2010.2

for Support of Young Scientists and Candidates of Science).

REFERENCES

1. A. Yu. Kazimirov, M. V. Koval'chuk, and V. G. Kon, *Kristallografiya* **39**, 258 (1994) [*Crystallogr. Rep.* **39**, 216 (1994)].
2. S. L. Chang, *Multiple Diffraction of X Rays in Crystals*. (Springer, Berlin, 1984; Mir, Moscow, 1987).
3. A. Kazimirov and V. G. Kohn, *Acta Crystallogr., Sect. A* **66**, 451 (2010).
4. A. E. Blagov, M. V. Koval'chuk, V. G. Kon, et al., *Kristallografiya* **55**, 12 (2010) [*Crystallogr. Rep.* **55**, 10 (2010)].
5. <http://www.kcsr.kiae.ru/stations/k6.6.php>
6. V. G. Kon, *Kristallografiya* **33**, 56 (1988) [*Sov. Phys. Crystallogr.* **33**, 30 (1988)].
7. R. Hoier and K. Martinsen, *Acta Crystallogr., Sect. A* **39**, 854 (1983).
8. V. G. Kohn, *Phys. Status Solidi A* **54**, 375 (1979).